

First-principles screening for sustainable OTS materials

S. Clima¹, D. Matsubayashi,¹ T. Ravsher^{1,2}, D. Garbin¹, R. Delhougne¹, G. S. Kar¹, G. Pourtois¹

¹imec, Kapeldreef 75, Leuven, Belgium

²KULeuven, Celestijnenlaan 200F, Leuven, Belgium

E-mail address of corresponding author: sergiu.clima@imec.be

Abstract — Chalcogenides Ovonic Threshold Switching (OTS) chalcogenide materials have suitable electronic properties for two-terminal selector application. To reduce the use of toxic elements, there is a need to replace As and Se of the presently-used OTS materials with environmentally friendly OTS materials. In an effort to accelerate the discovery of such materials, we predicted electrical device parameters only from atomistic first-principles simulations and performed a theoretical screening for alternative OTS compositions. With the help of the identified correlations between the theoretical trap/mobility gaps, the local atomic coordination environments and the experimentally-measured threshold, hold voltages or hold, leakage currents and other physics-based material parameter filters like material stability and OTS gauge, we identified more than 35 promising As/Se-free ternary alloy OTS compositions.

Keywords — Density functional theory, ovonic threshold switching, chalcogenides, material screening, selector.

1. Introduction

One of the most important challenges of the semiconductor industry is the need for sustainable materials, but the conventional ovonic threshold switching (OTS) materials [1] used in memory selector devices contain As and Se [2-6].

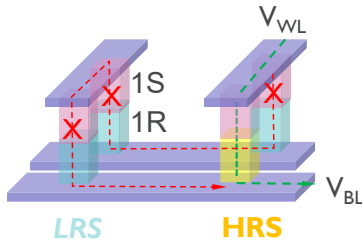


Fig. 1 SELECTOR device in series with resistive memory element (1S1R): cut the parasitic leakage on half-biased low-resistance-state memory cells, while allowing the correct reading of a high-resistance-state memory cell.

The ongoing efforts to develop two-terminal selector devices are directed towards suppressing the sneak-path leakage currents (Fig. 1). Ovonic Threshold Switching (OTS) materials seem very promising in that respect: at half of threshold voltage, the leakage current through the material is orders of magnitude lower (Fig. 2a) [1,7-9]. Aside from selector device, these materials can also be used for stand-alone self-rectified memory device [10,11]. For these two applications, the OTS material needs to correspond to different, but well-defined electrical specifications, hence there is a need to understand the material parameters and

correlate them to the device ones. In this respect, we investigated the exact relationships between atomic/electronic structure and experimental parameters on a series of OTS materials both from ab-initio and experimental point of view [12]. The identified relationships were used to screen for suitable materials only from theoretically-simulated material parameters. In this work we report the screened materials for two target applications: “RRAM selector” and “OTS memory” [10,11].

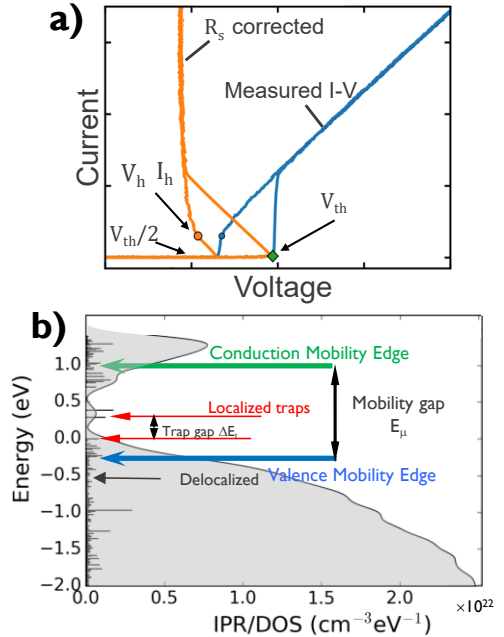


Fig. 2 a) I-V characteristics of an OTS MIM device b) Density of States (DOS) and Inverse Participation Ratio (IPR –horizontal bars) used to identify the mobility gap (E_μ) and the trap gap (ΔE_t).

2. Methodology

DFT computations: First-principles Density Functional Theory (DFT) simulations were performed with a Generalized Gradient Approximation (GGA/PBE) exchange-correlation functional using a mixed Gaussian and plane waves approach (GPW)[13]. The Brillouin zone was sampled only in the Γ -point. Atomic models were generated with a decorate-and-relax protocol [14]. The electronic properties were computed with a more accurate hybrid exchange-correlation functional (HSE06) to quantify the traps and mobility gaps. For the latter, we employed the inverse participation ratio (IPR)[15]. The reported electronic properties are median values over 10 different 2nm-sized amorphous models [12].

Experimental details: The experimental OTS (20nm) devices were fabricated with TiN as top and bottom electrodes in a mushroom-type cell structure,

deposited with a physical vapor deposition (PVD) technique. From a series of triangular ac pulses ($t_{\text{rise}}=10\mu\text{s}$ and amplitude 9V/7V for first-fire/switching), first-fire (V_{FF}) and threshold voltage (V_{th}) values were averaged over 10 dies. Also, the quenched defects (N_d) in the conduction cluster was extracted from the V_{th} distribution statistics [16].

2. Results and Discussions

We found positive correlations between the Density Function Theory computed mobility gap (Fig. 2b illustrates the DFT $E_{\mu}/\Delta E_t$ parameter extraction from the computed electronic structure of the material) and experimental first-fire (V_{FF})/threshold (V_{th}) / hold voltages (V_{h}) (Fig. 3) and hold current (I_{h} not shown). The reader should keep in mind that the presented correlations are not universal, only applicable to the available dataset and cannot be extrapolated to the literature data (the fabrication method/process, film thickness, electrical measurement parameters and DFT methodology to extract the mobility gap may yield different results).

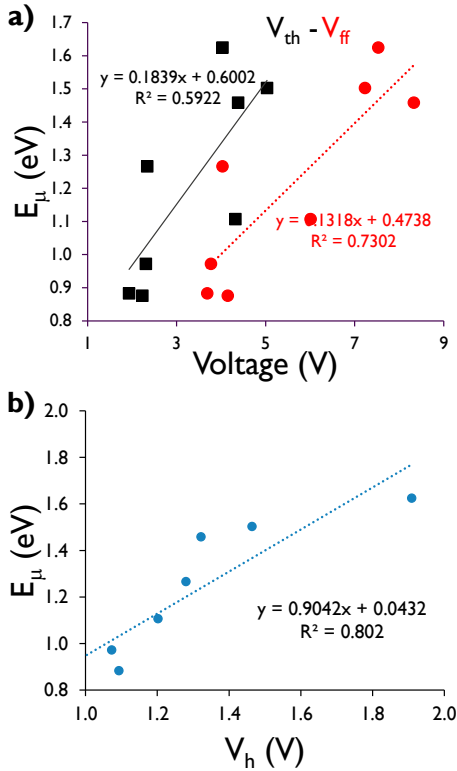


Fig. 3 DFT mobility gap (E_{μ}) correlates with a) experimental first-fire (red dots) and threshold voltages (black squares) and b) hold voltages.

The correlations with experimental leakage currents, extracted trap density and the theoretical local octahedral environment, on the other hand, were found to be negative (Fig. 4) [12].

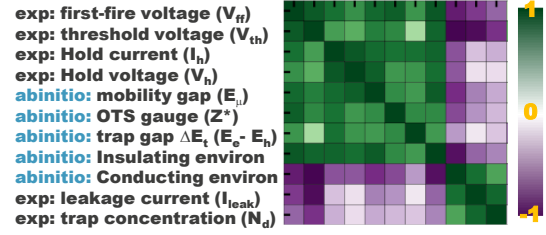


Fig. 4 Pearson correlation factor-coloured matrix shows cross-correlations between insulating and conductive sets of parameters.

In Fig. 5 we show that it is feasible to predict OTS behavior of the material, based only on first-principles simulated OTS gauge (a quantitative indicator for the OTS behavior of the material), that is derived from atomic Born effective charges [17-19].

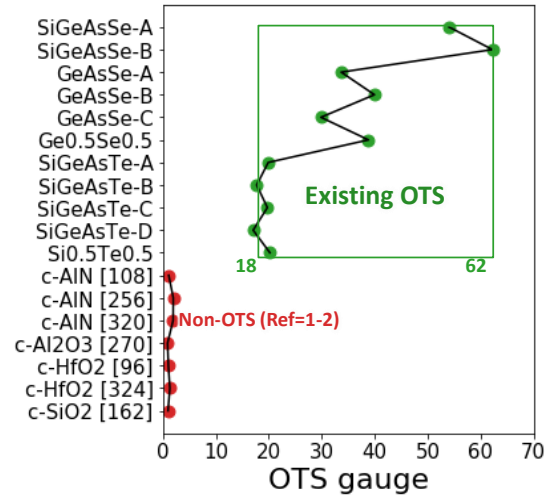


Fig. 5 DFT-computed OTS gauge for experimentally-known OTS materials is an order of magnitude higher than for non-OTS materials.

With this learning, we proceed to the screening for alternative ternary OTS materials exclusively from first-principles simulations [19]. More specifically, we focus only on ternary compounds and down-select only the OTS materials that pass through eight screening filters, to funnel down the large number of possible chemical compositions. As the title implies, we start by down-selecting the chemical elements that are not undesirable in the cleanroom, *i.e.*, excluded As, Se and Cd and include the top-right corner of the periodic table that should have appropriate hybridization/ionicity to form amorphous semiconducting alloys [20,21]: B, C, N, Al, Si, P, S, Zn, Ga, Ge, In, Sn, Sb and Te. Oxides were not included in this study, as they are subject of an ongoing investigation. From these 14 elements one can have more than 13000 ternary compositions with a 10% atomic fraction step. Only $\sim 1/9$ have OTS-suitable number of valence electrons (5 valence electrons rule [21]) and BEOL-compatible glass-transition temperature ($T_g > 600\text{K}$, Fig. 6). Hence only for these ~ 1400 compositions we generated amorphous models and computed the DFT

electronic structure, from which we extract the mobility gaps and trap gaps.

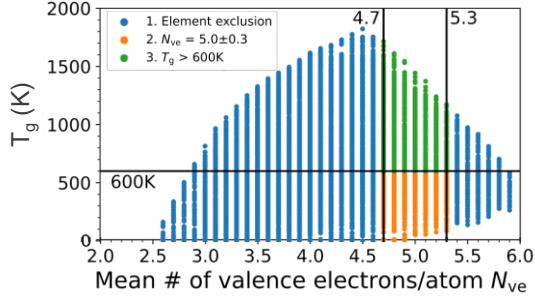


Fig. 6 Only compositions with glass-transition temperature $>600\text{K}$ and 5 ± 0.3 valence electrons/atom (green dots) were further considered for DFT simulations.

For a smaller subset of compositions that are thermodynamically stable (~ 420 compositions) with open electronic gap (~ 360 compositions Fig. 7), we also computed the Born effective charges to extract the OTS-gauge. The data cloud shows a trend of increased electronic gap with material stability. Fortunately, the gap of interest (around or below 1eV) does not include too low (stable/exothermic) formation energies, such that the material would be too stable with high trap formation energy (first-fire would correlate with the formation energy as well, if it correlates with the mobility gap, Fig. 3). Also, low formation energy would have a high thermodynamic driving force to stabilize the higher-energy amorphous atomic matrix, hence would present a reliability concern.

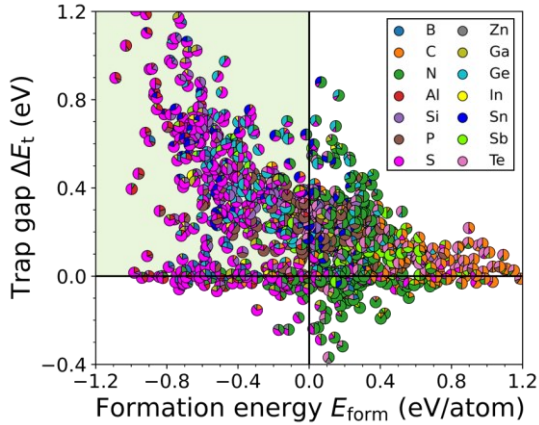


Fig. 7 Formation energy and the electronic gap of the ternary compositions (pie-chart dot representing the chemical composition). Only open gap and stable compositions (green area) were selected for further analysis.

For various applications one requires different electronic properties, which would deliver different threshold/ hold voltages or currents. For RRAM selector application we defined a specific mobility/trap gap, as shown in the Fig. 8. Other applications, like OTS memory, we relax the $0.25\text{-}0.2\text{eV}$ $E_{\mu}\text{-}\Delta E_t$ window to $0.7\text{-}0.5\text{eV}$, respectively.

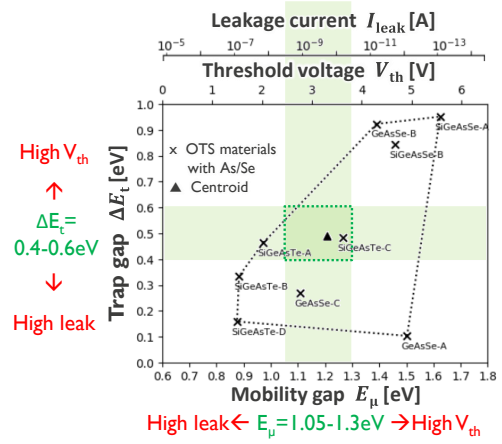


Fig. 8 $E_{\mu}\text{-}\Delta E_t$ window of interest for RRAM selector. $V_{th}/I_{leak}\text{-}E_{\mu}$ correlations are mapped on top axes

To investigate the materials ability to demix into simpler, lower energy sub-compositions/ phases, we estimated the spinodal temperature (Fig. 9) of the promising compositions and exclude the ones that will show instability against de-mixing, which should be a reliability issue.

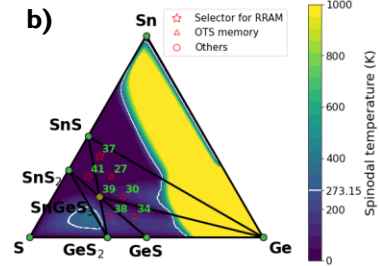


Fig. 9 Spinodal temperature for a list of Ge-Sn-S compositions.

After all filtering process, we identified the following ternary amorphous compositions that are supposed to behave as OTS materials, be stable at BEOL temperatures against demixing and show threshold voltages between $1\text{-}5\text{V}$ with leakage smaller than $1\mu\text{A}$.

	Composition
1	$\text{B}_{0.2}\text{P}_{0.5}\text{S}_{0.3}$
2	$\text{C}_{0.2}\text{S}_{0.5}\text{Sb}_{0.3}$
3	$\text{N}_{0.1}\text{S}_{0.6}\text{Sn}_{0.3}$
4	$\text{Al}_{0.3}\text{P}_{0.4}\text{S}_{0.3}$
5-10	$\text{Si}_{0.3\text{-}0.5}\text{P}_{0.1\text{-}0.5}\text{S}_{0.2\text{-}0.4}$
11-14	$\text{Si}_{0.1\text{-}0.5}\text{S}_{0.4\text{-}0.6}\text{Ge}_{0.1\text{-}0.5}$
15-17	$\text{Si}_{0.2\text{-}0.4}\text{S}_{0.4\text{-}0.5}\text{Sn}_{0.2\text{-}0.3}$
18-21	$\text{Si}_{0.4\text{-}0.5}\text{S}_{0.2\text{-}0.4}\text{Te}_{0.1\text{-}0.3}$
22-29	$\text{P}_{0.1\text{-}0.4}\text{S}_{0.3\text{-}0.5}\text{Ge}_{0.2\text{-}0.5}$
30	$\text{P}_{0.5}\text{S}_{0.4}\text{In}_{0.1}$
31-35	$\text{S}_{0.5\text{-}0.6}\text{Ge}_{0.1\text{-}0.4}\text{Sn}_{0.1\text{-}0.4}$

3. Conclusion

In the present work, we screened for ternary OTS-switching materials that can be used for RRAM selector or OTS memory application. Ternary combinations of 14 elements with 10% atomic fraction steps were pre-screened for the average number of valence electrons and estimated glass-transition temperature. The resulting compositions

were investigated with first-principles simulations. Further post-screening for OTS gauge and demixing identified more than 35 promising OTS materials that require experimental confirmation to validate our theoretical screening approach.

Acknowledgment

This work was carried out in the framework of the imec Core CMOS – Active Memory Program. T.R. thanks FWO for funding (grant no 1SD4721).

References

- [1] S. R. Ovshinsky, *Physical Review Letters* **21**, 1450 (1968).
- [2] S. Clima, D. Garbin, W. Devulder, J. Keukelier, K. Opsomer, L. Goux, G. S. Kar, and G. Pourtois, in *INFOS* 2019.
- [3] W. Devulder *et al.*, *Thin Solid Films* **753**, 139278 (2022).
- [4] D. Garbin *et al.*, in *65th IEEE Annual International Electron Devices Meeting (IEDM)* 2019.
- [5] S. Kabuyanagi *et al.*, in *IEEE Symposium on VLSI Technology and Circuits*, 2020.
- [6] A. Verdy, F. d'Acapito, J. B. Dory, G. Navarro, M. Bernard, and P. Noe, *Physica Status Solidi-Rapid Research Letters*, 1900548 (2019).
- [7] B. Govoreanu *et al.*, in *VLSI* 2017.
- [8] G. W. Burr, R. S. Shenoy, K. Virwani, P. Narayanan, A. Padilla, B. Kurdi, and H. Hwang, *Journal of Vacuum Science & Technology B* **32**, 040802 (2014).
- [9] S. Clima *et al.*, in *IEEE International Electron Devices Meeting (IEDM)* 2017.
- [10] T. Ravsher *et al.*, in *2022 IEEE Symposium on VLSI Technology and Circuits (VLSI Technology and Circuits)* 2022, pp. 312.
- [11] T. Ravsher *et al.*, *physica status solidi (RRL) – Rapid Research Letters* (2023).
- [12] S. Clima, T. Ravsher, D. Garbin, R. Degraeve, A. Fantini, R. Delhougne, G. S. Kar, and G. Pourtois, *ACS Applied Electronic Materials* **5**, 461 (2023).
- [13] T. D. Kuhne *et al.*, *Journal of Chemical Physics* **152**, 194103 (2020).
- [14] Y. Youn, Y. Kang, and S. Han, *Computational Materials Science* **95**, 256 (2014).
- [15] N. C. Murphy, R. Wortis, and W. A. Atkinson, *Physical Review B* **83**, 184206 (2011).
- [16] R. Degraeve, T. Ravsher, S. Kabuyanagi, A. Fantini, S. Clima, D. Garbin, G. S. Kar, and Ieee, in *IEEE International Reliability Physics Symposium (IRPS)* 2021, pp. 1.
- [17] J. Y. Raty and P. Noe, *Physica Status Solidi-Rapid Research Letters* **14**, 1900581 (2020).
- [18] P. Noe, A. Verdy, F. d'Acapito, J. B. Dory, M. Bernard, G. Navarro, J. B. Jager, J. Gaudin, and J. Y. Raty, *Science Advances* **6**, eaay2830 (2020).
- [19] D. Matsubayashi, S. Clima, T. Ravsher, D. Garbin, R. Delhougne, G. S. Kar, and G. Pourtois, in *2022 IEEE International Electron Devices Meeting (IEDM)* 2022.
- [20] A. Velea, K. Opsomer, W. Devulder, J. Dumortier, J. Fan, C. Detavernier, M. Jurczak, and B. Govoreanu, *Scientific Reports* **7**, 8103 (2017).
- [21] D. Lencer, M. Salinga, B. Grabowski, T. Hickel, J. Neugebauer, and M. Wuttig, *Nature Materials* **7**, 972 (2008).